

Synthesis and cellular studies of PEG-functionalized *meso*-tetraphenylporphyrins

Martha Sibrian-Vazquez, Timothy J. Jensen, M. Graça H. Vicente *

Department of Chemistry, Louisiana State University, 433 Choppin Hall, Baton Rouge, LA 70803, USA

Received 7 June 2006; received in revised form 3 August 2006; accepted 7 August 2006

Available online 20 September 2006

Abstract

The total syntheses of four PEG-functionalized porphyrins, containing one to four low molecular weight PEG chains linked via amide bonds to the *para*-phenyl positions of *meso*-tetraphenylporphyrin, are reported. The hydrophobic character of the PEG-porphyrins decreases with the number of PEG chains linked to the porphyrin ring, while their tendency for aggregation in buffered aqueous solution increases. The porphyrins containing one or two PEG chains accumulated within human HEP2 cells to a much higher extent than those having three or four PEGs at the macrocycle periphery. All PEG-porphyrins were found to be non-toxic in the dark, and only those containing one or two PEG chains were phototoxic ($IC_{50} = 2 \mu\text{M}$ at 1 J/cm^2 light dose). The preferential sites of subcellular localization of the porphyrins containing one or two PEG chains were found to be the mitochondria and endoplasmic reticulum (ER), while those containing three or four PEG chains localize preferentially in the lysosomes.

© 2006 Elsevier B.V. All rights reserved.

Keywords: Porphyrin; PEG; PDT; Cytotoxicity; Cellular uptake; Subcellular localization

1. Introduction

Photodynamic therapy (PDT) is a binary modality for cancer treatment that uses light to activate a tumor-localized photosensitizer, selectively destroying tumor tissue via the *in situ* generation of highly cytotoxic reactive oxygen species (e.g. $^1\text{O}_2$) [1,2]. This technique has advantages over other cancer treatment modalities, such as surgery, radio- and chemo-therapy, because it has the potential to selectively target malignant vs. normal cells. Therefore, the biological efficacy of the PDT treatment strongly depends on the specific delivery of a photosensitizer to tumor tissue in order to avoid undesirable normal tissue damage, such as skin photosensitivity. Most of the currently available photosensitizers are highly hydrophobic compounds, often with long retention times (i.e. weeks)

in tissues and difficult to formulate [3,4]. Recently, several strategies have been developed to improve the solubility and tumor-specificity of PDT photosensitizers, including their conjugation to carrier proteins [5–7], oligonucleotides [8,9], monoclonal antibodies [10–12], epidermal growth factors [13,14], carbohydrates [15,16], and hydrophilic polymers [17–19]. The use of polyethylene glycol (PEG) as a carrier or covalently attached to drugs is another commonly used strategy for drug delivery to target sites [20–22]. The pegylation of porphyrin-based photosensitizers has been used to improve their serum life, to reduce their uptake by the reticuloendothelial system, and to increase their tumor accumulation and water-solubility [23]. Several *in vitro* and *in vivo* studies have been reported on the PEG conjugates of chlorin e_6 [23], *meta*-tetrahydroxyphenylchlorin (*m*THPC) [24–29], protoporphyrin IX [30,31], hematoporphyrin IX [32–34], and benzoporphyrins [35–37]. In general, covalently linked PEG-photosensitizers have shown increased tumor selectivity, in both *in vitro* and *in vivo* studies. However, the phototoxic effect of the

* Corresponding author. Tel.: +1 225 578 7405; fax: +1 225 578 3458.
E-mail address: vicente@lsu.edu (M. Graça H. Vicente).

PEG-functionalized photosensitizers depends significantly on the length of the PEG chain, the nature of the linkage between the PEG and the photosensitizer, and on the overall molecular charge and its aggregation behavior. Most studies reported to date involve high molecular weight PEGs (2000–10,000 amu), and as a result mixtures of high molecular weight PEG-photosensitizer conjugates were obtained due to the polydispersity of the PEGs (M_w/M_n 1.01 for PEGs < 5 kDa and 1.1 for PEGs > 50 kDa). Furthermore, because of the flexibility of the PEG chain and its association with water molecules (approximately 2–3 water molecules per ethylene oxide unit), the PEG-photosensitizers often behave as molecules of very high molecular weight and large size, about 5–10 times larger than, for example, a protein of similar molecular mass [21]. We have recently used a low molecular weight PEG linker in the preparation of a series of porphyrin-peptide conjugates [38]. In our continuing studies of structure/activity relationships and the biological efficacy of porphyrin-based photosensitizers, we now report the syntheses of a series of PEG-functionalized photosensitizers, containing one to four low molecular weight PEG chains covalently linked to the porphyrin macrocycle, and the evaluation of their *in vitro* biological properties using human HEP2 cells. Our studies show that low molecular weight PEG-functionalized porphyrins can be efficiently synthesized and that their biological efficacy depends on the number of PEG chains linked to the porphyrin periphery.

2. Experimental

All commercially available starting materials were used directly without further purification, unless otherwise indicated. All reactions were monitored by TLC using Sorbent Technologies 0.25 mm silica gel plates with UV indicator (60F-254), fractions being visualized by staining with iodine. Silica gel Sorbent Technologies 32–63 μm was used for flash column chromatography. ^1H NMR spectra were obtained on either a DPX-250 or a ARX-300 Bruker spectrometer. Chemical shifts (δ) are given in parts per million relative to CDCl_3 (7.26 ppm, ^1H) unless otherwise indicated. Electronic absorption spectra were measured on a Perkin Elmer Lambda 35 UV–Vis spectrophotometer and fluorescence spectra were measured on a Perkin Elmer LS55 spectrometer. Mass spectra were obtained on an Applied Biosystems QSTAR XL, a hybrid QqTOF mass spectrometer with a MALDI ionization source using CCA as the matrix. HPLC analysis was carried out on a Dionex system including a P680 pump and a UVD340U, detector. Analytical HPLC was carried out using a Delta Pak C_{18} 300 Å, 5 μm , 3.9 \times 150 mm (Waters, USA) column and a stepwise gradient 5–95% Buffer B. Buffer A (5% acetonitrile, 0.1% TFA, H_2O), buffer B (5% H_2O , 0.1% TFA, acetonitrile). 5,10,15,20-Tetra(4-aminophenyl)porphyrin was purchased from TCI. The 5-(4-aminophenyl)-10,15,20-triphenylporphyrin, 5,10-di(4-aminophenyl)-15,20-diphenylporphyrin and 5,10,15-tri(4-aminophenyl)-20-phenylporphyrin were synthesized

by nitration of 5,10,15,20-tetraphenylporphyrin (TPP) using NaNO_2/TFA followed by reduction with SnCl_2/HCl , as previously described [38].

For the cell culture experiments, all tissue culture media and reagents were obtained from Invitrogen. Human HEP2 cells were obtained from ATCC and maintained in a 50:50 mixture of DMEM:Advanced MEM containing 5% FBS. The cells were sub-cultured biweekly to maintain sub-confluent stocks.

2.1. 5-[4-(*N*-Glycolic acid-amino)phenyl]-10,15,20-triphenylporphyrin (**2**)

To a solution of 5-(4-aminophenyl)-10,15,20-triphenylporphyrin (0.317 mmol) in DMF (1 mL) was added diglycolic anhydride (0.476 mmol) and the final solution was stirred at room temperature overnight. The reaction mixture was diluted with 10 mL of CHCl_3 , followed by addition of hexanes until precipitation occurred. The precipitate was filtered and washed with water to remove residual anhydride, and then dried under vacuum to yield 0.237 g (100%) of porphyrin **2**. UV–Vis (CHCl_3) λ_{max} ($\epsilon/\text{M}^{-1}\text{cm}^{-1}$) 414 (406,000), 512 (16,900), 547 (9000), 589 (5400), 645 (4100). ^1H NMR ($\text{DMSO}-d_6$, 300 MHz): δ 10.39 (1H, s), 8.82–8.90 (8H, m), 8.10–8.31 (10H, m), 7.82–7.84 (9, m), 4.36 (2H, s), 4.34 (2H, s), –2.91 (2H, s). HRMS (MALDI) m/z 746.2799 ($\text{M}+\text{H}^+$), calculated for $\text{C}_{48}\text{H}_{35}\text{N}_5\text{O}_4$ 746.2689.

2.2. 5,10-Di[4-(*N*-glycolic acid-amino)phenyl]-15,20-diphenylporphyrin (**3**)

The title porphyrin was synthesized as described above for porphyrin **2**, using 5,10-di(4-aminophenyl)-15,20-diphenylporphyrin (0.031 mmol) and glycolic anhydride (0.093 mmol) in 1 mL of DMF. Porphyrin **3** was obtained in 99% yield (0.027 g). UV–Vis (MeOH) λ_{max} ($\epsilon/\text{M}^{-1}\text{cm}^{-1}$) 421 (381,400), 517 (26,400), 553 (16,500), 591 (10,000), 648 (8600). ^1H NMR (acetone- d_6 , 300 MHz): δ 9.98 (2H, s), 8.92 (4H, s), 8.84 (4H, s), 8.19 (12H, s), 7.82 (6H, s), 4.48 (4H, s), 4.42 (4H, s), –2.81 (2H, s). HRMS (MALDI) m/z 877.3001 ($\text{M}+\text{H}^+$), calculated for $\text{C}_{52}\text{H}_{40}\text{N}_6\text{O}_8$ 877.2908.

2.3. 5,10,15-Tri[4-(*N*-glycolic acid-amino)phenyl]-20-phenylporphyrin (**4**)

The title porphyrin was synthesized as described above for porphyrin **2**, using 5,10,15-tri(4-aminophenyl)-20-phenylporphyrin (0.060 mmol) and glycolic anhydride (0.363 mmol) in 1 mL of DMF. Porphyrin **4** was obtained in 93% yield (0.057 g). UV–Vis (MeOH) λ_{max} ($\epsilon/\text{M}^{-1}\text{cm}^{-1}$) 417 (409,300), 515 (18,700), 551 (13,600), 590 (8700), 647 (7800). ^1H NMR ($\text{DMSO}-d_6$, 300 MHz): δ 10.37 (3H, s), 8.80–8.87 (8H, m), 8.09–8.22 (12H, m), 7.68 (3H, s), 4.33–4.35 (12H, m), –2.84 (2H, s). LRMS (MALDI) m/z 1008.594 ($\text{M}+\text{H}^+$), calculated for $\text{C}_{56}\text{H}_{45}\text{N}_7\text{O}_{12}$ 1008.9962.

2.4. 5,10,15,20-Tetra[4-(*N*-glycolic acid-amino)phenyl]-porphyrin (**5**)

The title porphyrin was synthesized as described above for porphyrin **2**, using 5,10,15,20-Tetra(4-aminophenyl)porphyrin (0.030 mmol) and glycolic anhydride (0.240 mmol) in 1 mL of DMF. Porphyrin **5** was obtained in 95% yield (0.032 g). UV–Vis (MeOH) λ_{\max} ($\epsilon/\text{M}^{-1} \text{cm}^{-1}$) 418 (407,300), 515 (16,100), 551 (11,500), 591 (5800), 648 (6200). ^1H NMR (DMSO- d_6 , 300 MHz): δ 10.35 (4H, s), 8.84–8.87 (6H, m), 8.02–8.12 (12H, m), 4.31–4.33 (16H, m), –2.92 (2H, s). LRMS (MALDI) m/z 1138.561 (M^+), calculated for $\text{C}_{60}\text{H}_{50}\text{N}_8\text{O}_{16}$ 1138.3345.

2.5. 5-(4-PEGphenyl)-10,15,20-triphenylporphyrin (**6**)

To a solution of porphyrin **2** (0.100 g, 0.134 mmol) in DMF (1 mL) were added Et_3N (0.081 g, 0.804 mmol) and HOBt (0.020 g, 0.134 mmol). After stirring the mixture for 5 min $\text{NH}_2\text{CH}_2\text{CH}_2(\text{OCH}_2\text{CH}_2)_5\text{OCH}_2\text{CO}_2^t\text{Bu}$ (0.053 g, 0.134 mmol) was added followed by EDCI (0.026 g, 0.134 mmol) and stirring continued for 48 h at room temperature. The reaction mixture was diluted with 50 mL of ethyl acetate, washed with water (3×100 mL), dried over anhydrous Na_2SO_4 , and the solvent evaporated under vacuum. The target porphyrin was purified by flash chromatography on silica gel using ethyl acetate followed by ethyl acetate:methanol 90:10 for elution. The *tert*-butyl ester of porphyrin **6** was obtained in 64% yield (0.193 g). UV–Vis (CHCl_3) λ_{\max} ($\epsilon/\text{M}^{-1} \text{cm}^{-1}$) 419 (452,700), 516 (17,400), 551 (8800), 590 (5600), 646 (4300). ^1H NMR (CDCl_3 , 300 MHz): δ 8.89–8.95 (5H, m), 8.24–8.26 (6H, m), 8.15 (2H, d, $J = 8.16$ Hz), 7.77–7.78 (9H, m), 7.61 (1H, s), 4.42 (2H, s), 4.33 (2H, s), 4.02 (2H, s), 3.66–3.68 (24H, m), 1.48 (9H, s), –2.70 (2H, s). HRMS (MALDI) m/z ($\text{M}+\text{H}^+$) 1123.5199, calculated for $\text{C}_{66}\text{H}_{70}\text{N}_6\text{O}_{11}$ 1122.5103. To a solution of the *tert*-butyl ester of porphyrin **6** in 1 mL of dichloromethane was added 1 mL of TFA and the final mixture was stirred at room temperature for 4 h. After removal of the solvent under vacuum, the residue was triturated, washed with diethyl ether and dried under vacuum to give the title porphyrin **6** in quantitative yield. HPLC, $t_r = 17.05$ min. UV–Vis (CHCl_3) λ_{\max} ($\epsilon/\text{M}^{-1} \text{cm}^{-1}$) 421 (354,400), 513 (15,000), 549 (7200), 589 (4500), 645 (3300). ^1H NMR (CDCl_3 , 300 MHz): δ 8.72–8.74 (8H, m), 8.61–8.63 (8H, m), 8.37 (2H, d, $J = 8.28$ Hz), 7.98–8.07 (10H, m), 4.48 (2H, s), 4.41 (2H, s), 4.17 (2H, s), 3.68–3.72 (24H, m), –0.68 (2H, s). HRMS (MALDI) m/z ($\text{M}+\text{H}^+$) 1067.4586, calculated for $\text{C}_{62}\text{H}_{63}\text{N}_6\text{O}_{11}$ 1067.4554.

2.6. 5,10-Di(4-PEGphenyl)-15,20-diphenylporphyrin (**7**)

The title porphyrin was synthesized as described above for porphyrin **6**, using porphyrin **3** (0.031 mmol) and $\text{NH}_2\text{CH}_2\text{CH}_2(\text{OCH}_2\text{CH}_2)_5\text{OCH}_2\text{CO}_2^t\text{Bu}$ (0.062 mmol). The *tert*-butyl ester of porphyrin **7** was obtained in 54%

yield (0.025 g). UV–Vis (CHCl_3) λ_{\max} ($\epsilon/\text{M}^{-1} \text{cm}^{-1}$) 421 (390,800), 517 (15,000), 552 (9200), 591 (5800), 647 (4800). ^1H NMR (CDCl_3 , 300 MHz): δ 8.84–8.92 (8H, m), 8.18–8.26 (8H, m), 8.09–8.13 (4H, m), 7.75–7.77 (8H, m), 7.55 (2H, s), 4.37 (4H, s), 4.30 (4H, s), 3.99 (4H, s), 3.62–3.68 (60H, m), 1.48 (18H, s), –2.76 (2H, s). HRMS (MALDI) m/z 1631.456 ($\text{M}+\text{H}^+$), calculated for $\text{C}_{88}\text{H}_{110}\text{N}_8\text{O}_{22}$ 1631.7735. Deprotection of the *tert*-butyl group as described above gave porphyrin **7** in quantitative yield (0.016 g). HPLC $t_r = 15.51$ min. UV–Vis (CHCl_3) λ_{\max} ($\epsilon/\text{M}^{-1} \text{cm}^{-1}$) 421 (365,600), 516 (19,200), 553 (14,000), 591 (9500), 648 (9000). ^1H NMR (CDCl_3 , 300 MHz): δ 10.06 (2H, s), 8.56–8.59 (16H, m), 8.30–8.40 (4H, m), 7.97–8.01 (8H, m), 7.73 (2H, s), 4.38 (4H, s), 4.30 (4H, s), 4.01 (4H, s), 3.62–3.68 (60H, m). LRMS (MALDI) m/z 1518.465 (M^+), calculated for $\text{C}_{80}\text{H}_{94}\text{N}_8\text{O}_{22}$ 1518.6483.

2.7. 5,10,15-Tri(4-PEGphenyl)-20-phenylporphyrin (**8**)

The title porphyrin was synthesized as described above for porphyrin **6**, using porphyrin **4** (0.030 mmol) and $\text{NH}_2\text{CH}_2\text{CH}_2(\text{OCH}_2\text{CH}_2)_5\text{OCH}_2\text{CO}_2^t\text{Bu}$ (0.098 mmol). The *tert*-butyl ester of porphyrin **8** was obtained in 61% yield (0.039 g). UV–Vis (CHCl_3) λ_{\max} ($\epsilon/\text{M}^{-1} \text{cm}^{-1}$) 422 (380,200), 517 (15,000), 554 (9700), 591 (5400), 648 (4700). ^1H NMR (CDCl_3 , 300 MHz): δ 8.83–8.88 (8H, m), 8.17–8.22 (8H, m), 8.08–8.11 (4H, m), 7.74–7.76 (2H, m), 7.52–7.59 (3H, m), 4.37 (6H, s), 4.30 (6H, s), 3.98 (6H, m), 3.59–3.67 (74H, m), 1.47 (27H, s), –2.77 (2 H, s). LRMS (MALDI) m/z 2137.100 (M^+), calculated for $\text{C}_{110}\text{H}_{150}\text{N}_{10}\text{O}_{33}$ 2139.0367. Deprotection of the *tert*-butyl group as described above gave porphyrin **8** in quantitative yield. HPLC $t_r = 12.62$ min. UV–Vis (CHCl_3) λ_{\max} ($\epsilon/\text{M}^{-1} \text{cm}^{-1}$) 423 (347,600), 517 (18,300), 554 (14,500), 591 (9200), 649 (9200). ^1H NMR (CDCl_3 , 300 MHz): δ 10.06 (3H, s) 8.73–8.88 (16H, m), 8.41–8.43 (6H, m), 8.02–8.04 (4H, m), 7.73 (3H, s), 4.42 (6H, s), 4.34 (6H, s), 4.09 (6H, s), 3.69–3.72 (74H, m). LRMS (MALDI) m/z 1970.286 (M^+), calculated for $\text{C}_{98}\text{H}_{126}\text{N}_{10}\text{O}_{33}$ 1970.8489.

2.8. 5,10,15,20-Tetra(4-PEGphenyl)porphyrin (**9**)

The title porphyrin was synthesized as described above for porphyrin **6**, using porphyrin **5** (0.017 mmol) and $\text{NH}_2\text{CH}_2\text{CH}_2(\text{OCH}_2\text{CH}_2)_5\text{OCH}_2\text{CO}_2^t\text{Bu}$ (0.105 mmol). The *tert*-butyl ester of porphyrin **9** was obtained in 40% yield (0.018 g). UV–Vis (CHCl_3) λ_{\max} ($\epsilon/\text{M}^{-1} \text{cm}^{-1}$) 423 (394,100), 519 (16,300), 555 (11,800), 592 (6500), 647 (6600). ^1H NMR (CDCl_3 , 300 MHz): δ 8.86 (6H, s), 8.16–8.19 (6H, m), 8.07–8.10 (6H, m), 7.46 (4H, s), 4.37 (8H, s), 4.16 (8H, s), 3.98 (8H, s), 3.52–3.67 (100H, m), –2.77 (2H, s). LRMS (MALDI) m/z 2646.42 ($\text{M}+\text{H}^+$), calculated for $\text{C}_{132}\text{H}_{190}\text{N}_{12}\text{O}_{44}$ 2647.2999. Deprotection of the *tert*-butyl group as described above gave porphyrin **9** in quantitative yield (0.015 g). HPLC $t_r = 11.20$ min. UV–Vis (CHCl_3) λ_{\max} ($\epsilon/\text{M}^{-1} \text{cm}^{-1}$) 424 (351,100), 518 (18,700), 555 (16,500), 593 (9800), 650 (10,000). ^1H NMR

(CDCl₃, 300 MHz): δ 10.06 (4H, s), 8.54 (16H, s), 8.35–8.38 (8H, m), 7.77 (4H, s), 4.37 (8H, s), 4.29 (8H, s), 4.14 (8H, s), 3.68–3.57 (100H, m). LRMS (MALDI) m/z 2424.047 (M⁺), calculated for C₁₁₆H₁₅₈N₁₂O₄₄ 2424.5497.

2.9. Time-dependent cellular uptake

HEp2 cells were plated at 10,000 per well in a Costar 96 well plate and allowed to grow 36 h. Porphyrin stock solutions (10 mM) were prepared in DMSO and then diluted into medium to final working concentrations. The cells were exposed to 10 μ M of each conjugate for 0, 1, 2, 4, 8, and 24 h. At the end of the incubation time, the loading medium was removed and the cells were washed with PBS pH 7.4. The cells were solubilized by addition of 100 μ L of 0.25% Triton X-100 (Calbiochem) in PBS. To determine the conjugate concentration, fluorescence emission was read at 440/650 nm (excitation/emission) using a BMG FLUOstar plate reader. The cell numbers were quantified using the CyQuant reagent (Molecular Probes).

2.10. Dark cytotoxicity

The HEp2 cells were plated as described above and allowed 36 h to attach. The cells were exposed to increasing concentrations of porphyrin up to 250 μ M and incubated overnight. The loading medium was then removed and the cells washed with growth medium and then fed medium containing Cell Titer Blue (Promega) as per manufacturer's instructions was added and incubated 4 h. Cell viability was then measured by reading the fluorescence at 520/584 nm using a BMG FLUOstar plate reader. The signal was normalized to 100% viable (untreated) cells and 0% viable (treated with 0.2% saponin from Sigma) cells.

2.11. Phototoxicity

The HEp2 cells were prepared as described above for the dark cytotoxicity assay, treated with porphyrin concentrations of 0, 1.25, 2.5, 5, and 10 μ M and incubated 24 h. The medium was removed and the cells washed twice with growth medium and fed 100 μ L of medium containing 50 mM HEPES pH 7.4. The cells were then placed on ice and exposed to light from a 100 W halogen lamp filtered through a 610 nm long pass filter (Chroma) for 20 min. An inverted plate lid filled with cold water to a depth of 5 mm acted as an IR filter. The total light dose was approximately 1 J/cm². The cells were returned to the incubator overnight and assayed for viability as described above for the dark cytotoxicity experiment.

2.12. Intracellular localization

The HEp2 cells were plated on LabTek 2 chamber coverslips and incubated overnight, before being exposed to 10 μ M of PEG-porphyrin for 18 h. For the co-localization experiments the cells were incubated for 18 h concur-

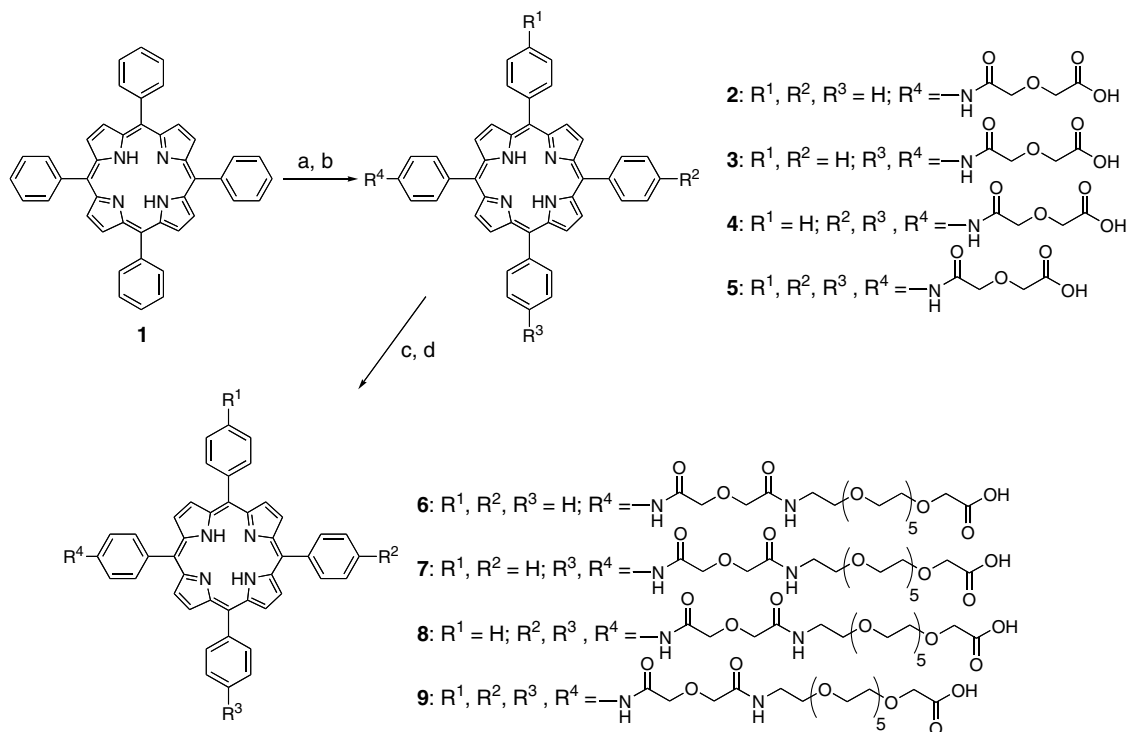
rently with porphyrin and one of the following organelle tracers, for 30 min: mitochondria were visualized using MitoTracker Green FM at 250 nM, lysosomes with Lyso-Sensor Green DND-189 at 50 nM, and ER with 50 nM of DiOC₆ 5 μ g/mL. The slides were washed three times with growth medium and new medium containing 50 mM HEPES pH 7.4 was added. Fluorescence microscopy was performed using a Zeiss Axiovert 200 M inverted fluorescence microscope fitted with standard FITC and Texas Red filter sets (Chroma). The images were acquired with a Zeiss AxioCam MRM CCD camera fitted to the microscope.

3. Results

3.1. Syntheses and structural characterization

The four PEG-functionalized porphyrins **6–9** were obtained from TPP (**1**) in just four steps, as shown in Scheme 1. TPP was regioselectively nitrated at the *para*-phenyl positions using NaNO₂/TFA, as previously reported [39]. Reduction of the nitro to amino groups with SnCl₂/HCl gave the mono-, di- and tri-aminoTPP derivatives in 35–53% overall yields. The tetra-aminoTPP was on the other hand obtained from a commercial source, since the corresponding tetra-nitroTPP is poorly soluble in organic solvents and usually isolated in low yields. The aminoTPP derivatives reacted with glycolic anhydride in DMF to give the carboxylic acid-functionalized porphyrins **2–5** in 93–100% yields. The conjugation of porphyrins **2–5** with hexa-ethylene glycol was achieved upon reaction with NH₂CH₂CH₂(OCH₂CH₂)₅OCH₂COO^tBu, which was prepared as we have previously described [38]. The hydroxybenzotriazole esters of porphyrins **2–5** reacted with NH₂CH₂CH₂(OCH₂CH₂)₅OCH₂COO^tBu in the presence of EDCI and Et₃N, to give the target porphyrins in 40–64 % yields. Deprotection using TFA/CHCl₃ gave PEG-functionalized porphyrins **6–9** in quantitative yields. While the mono- and di-PEG-porphyrins **6** and **7** are highly soluble in organic solvents and poorly soluble in water, the tri- and tetra-PEG derivatives **8** and **9** show good solubility in both water and in polar organic solvents, such as chloroform, ethyl acetate, methanol and acetone.

The PEG-functionalized porphyrins **6–9** were structurally characterized using ¹H NMR, MS, UV–Vis and fluorescence spectroscopy. In particular the fluorescence properties of porphyrins are often used to study their aggregation behavior in solution since porphyrins in their monomeric form normally show intense fluorescence emissions, which are partially or completely quenched upon aggregation in solution [40,41]. As shown in Fig. 1a–d, PEG-functionalized porphyrins **6–9** all exhibited intense fluorescence emissions between 651 and 656 nm, upon excitation within the Soret band, when dissolved in DMSO. However, whereas the fluorescence emissions for PEG-porphyrins **6** and **7** in 50 mM HEPES buffer (pH 7.4) remained unchanged (Fig. 1a and b), those for PEG-porphyrins **8**



Scheme 1. (a) $NaNO_2/TFA$ then $SnCl_2/HCl$, $65^\circ C$ (35–53%); (b) glycolic anhydride, DMF, rt, 24 h (93–100%); (c) $NH_2CH_2CH_2(OCH_2CH_2)_5OCH_2COO^tBu/HOBt/EDCI/Et_3N/DMF$, rt, 48 h (40–64% yield); (d) $CHCl_3/TFA$ 1:3, rt, 4 h (100%).

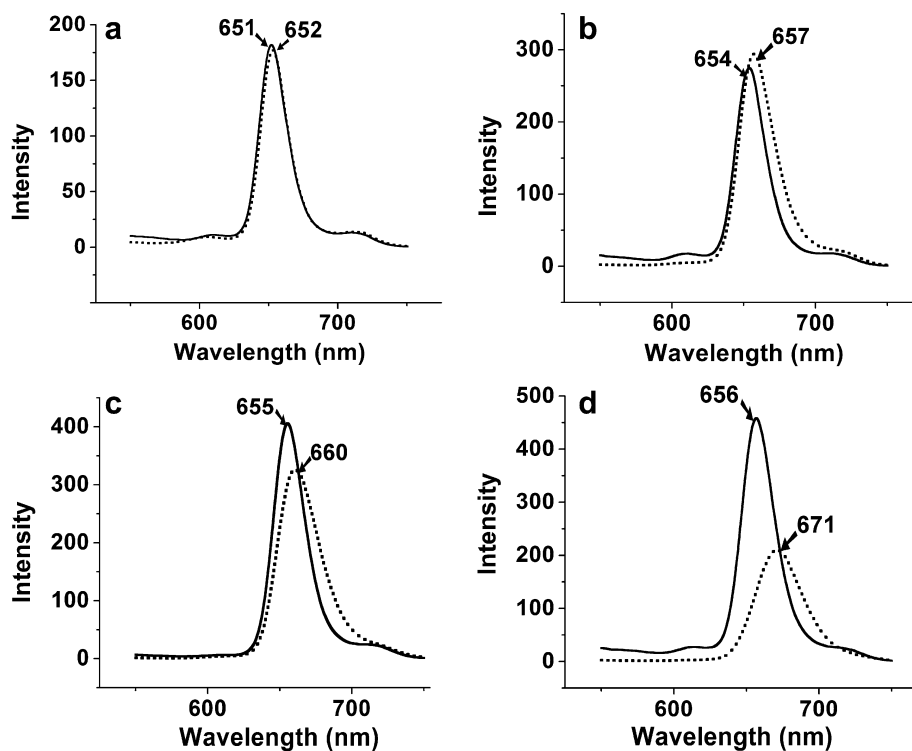


Fig. 1. Fluorescence emission spectra for PEG-porphyrins (a) **6**, (b) **7**, (c) **8** and (d) **9** at $10\ \mu M$ in DMSO (full line) and in 50 mM HEPES buffer, pH 7.4 (dotted line). Excitation at 440 nm.

and **9** showed a significant reduction in the fluorescence intensity, especially for the tetra-PEG-porphyrin **9**, along with broadening and red shift of the fluorescence emission

band (Fig. 1c and d). These results suggest that at the concentrations studied the PEG-porphyrins **8** and **9** aggregate in aqueous solution while porphyrins **6** and **7** do not.

3.2. Time-dependent uptake

The time-dependent cellular uptake of PEG-functionalized porphyrins 6–9 was evaluated in human HEP2 cells at a 10 μM porphyrin concentrations, and the results are shown in Fig. 2. The cellular uptake was dependent on the number of PEG chains at the porphyrin periphery. While porphyrins 6 and 7 were the most taken-up by the HEP2 cells, the more hydrophilic porphyrins 8 and 9 accumulated the least within cells. All conjugates exhibited similar uptake kinetics in the first 1–2 h. However, while the uptake of porphyrins 8 and 9 reached a plateau after 2 h, that of porphyrins 6 and 7 continuously increased overtime and after 24 h the amount of porphyrins 6 and 7 found within cells was 12-fold higher than that of porphyrins 8 and 9. Porphyrin 7, containing two PEG chains on adjacent *meso*-phenyl rings, accumulated the most within HEP2 cells of all porphyrins studied, while porphyrin 9 with four PEG chains accumulated the least.

3.3. Cytotoxicity

The dark- and photo-toxicity of the PEG-functionalized porphyrins 6–9 were investigated in human HEP2 cells exposed to increasing concentrations of each porphyrin for 24 h. The results are shown in Figs. 3 and 4, respectively. All PEG-porphyrins were found to be non-toxic in the dark at concentrations up to 250 μM using a Cell Titer Blue assay. Upon exposure to low light dose (1 J/cm^2) PEG-porphyrins 8 and 9 showed no toxicity at concentration up to 10 μM , while PEG-porphyrins 6 and 7 were found to be phototoxic, with determined IC_{50} values of 2.0 and 1.8 μM , respectively.

3.4. Intracellular localization

The subcellular localization of the PEG-functionalized porphyrins 6–9 was investigated by fluorescence microscopy, using human HEP2 cells. Figs. 5–8 show the fluorescent patterns observed for PEG-porphyrins 6–9, respectively, and

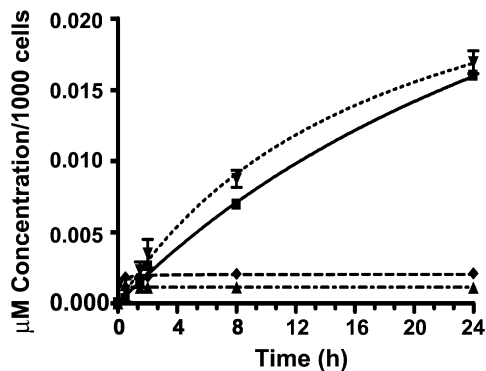


Fig. 2. Time-dependent uptake of PEG-porphyrins 6 (■, full line), 7 (▼, dotted line), 8 (◆, dashed line), 9 (▲, dot-dash line) at 10 μM by human HEP2 cells.

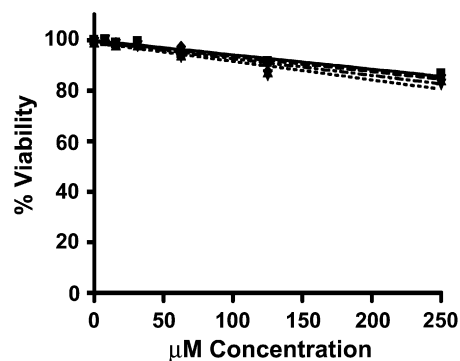


Fig. 3. Dark cytotoxicity of PEG-porphyrins 6 (■, full line), 7 (▼, dotted line), 8 (◆, dashed line), 9 (▲, dot-dash line) toward human HEP2 cells using the Cell Titer Blue assay.

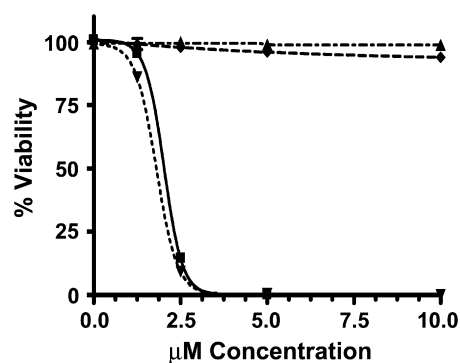


Fig. 4. Phototoxicity of PEG-porphyrins 6 (■, full line), 7 (▼, dotted line), 8 (◆, dashed line), 9 (▲, dot-dash line) toward human HEP2 cells at 1 J/cm^2 light dose.

their overlay with the organelle specific fluorescent probes DiOC₆ (ER), LysoSensor Green (lysosomes), and Mitotracker Green (mitochondria). The preferential sites of subcellular localization for PEG-porphyrins 6 and 7 were found to be the ER and the mitochondria, while for 8 and 9 were the cell lysosomes. Porphyrin 8 was also found in mitochondria. While PEG-porphyrins 6 and 7 showed an intense fluorescence signal for co-localization within the ER and mitochondria, PEG-porphyrins 8 and 9 showed a decreased intensity signal, probably as a result of their lower cellular uptake (see Fig. 2).

4. Discussion

4.1. Syntheses

Several methodologies have been used to prepare covalently linked PEG-drugs, bearing either strong or weak linkages between the PEG and the drug moieties [20–22]. Whereas weak PEG-drug linkages are normally used in the preparation of controlled-release drug formulations, strong linkages are preferred for hydrolytically stable conjugates. PEG-photosensitizers bearing carbamate, triazine, and amide bonds have been synthesized and it was

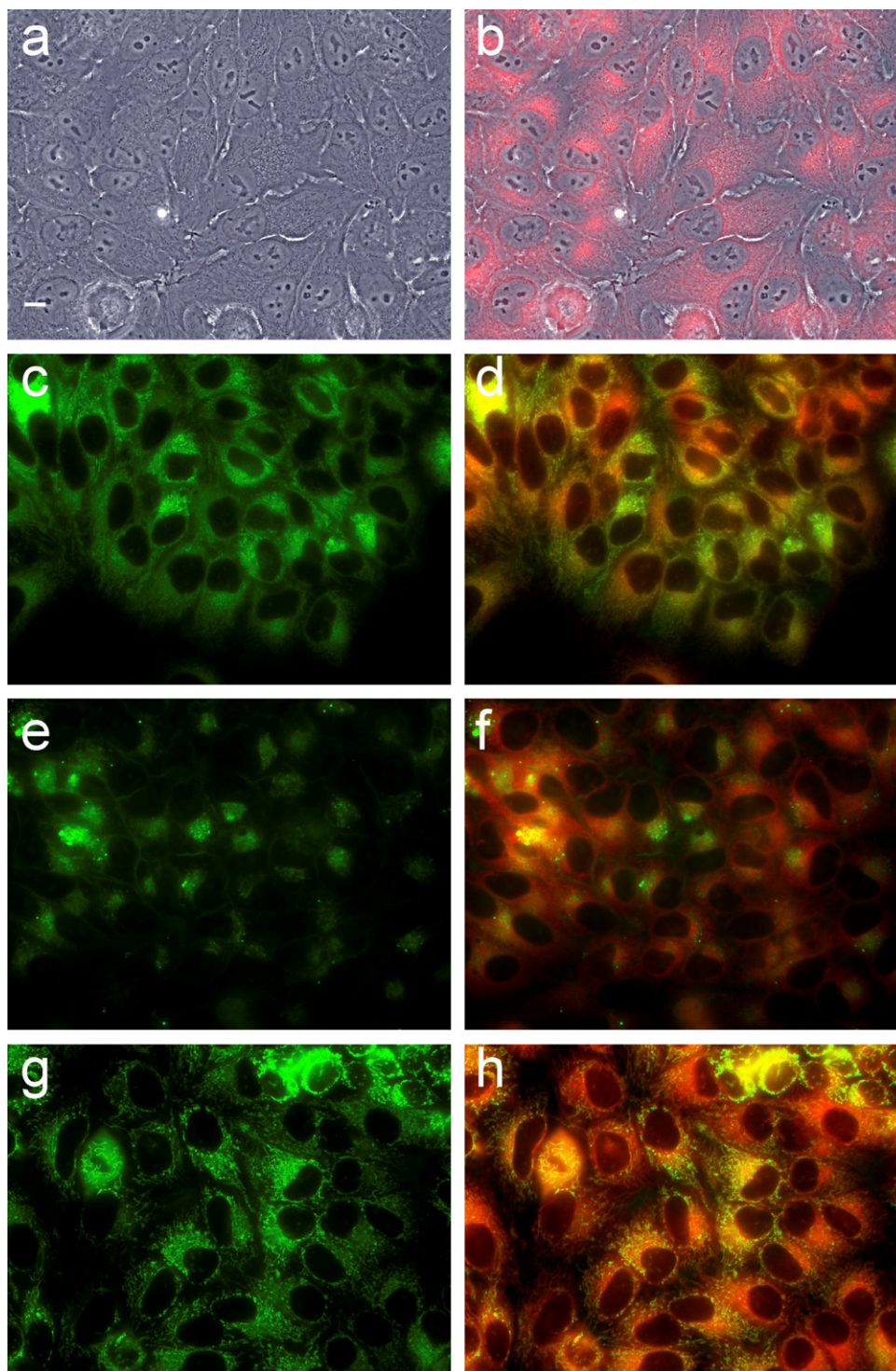


Fig. 5. Subcellular localization of conjugate **6** in HEP2 cells at 10 μ M for 18 h: (a) phase contrast, (b) overlay of **6** fluorescence and phase contrast, (c) DiOC₆ fluorescence, (e) LysoSensor Green fluorescence, (g) MitoTracker Green fluorescence, (d), (f), (h) overlays of organelle tracers with **6** fluorescence. Scale bar: 10 μ m.

reported that while the carbamate-linked sensitizers are easily hydrolyzed under physiological conditions, the triazine- and amide-linked molecules are significantly more stable under these conditions [42]. The methodologies normally used for the synthesis of PEG-sensitizers involve acylation reactions, Schiff base formation followed by

reduction, or sulfide bond formation [20–22]. Our PEG-functionalized porphyrins **6–9** were prepared via acylation reactions, and all contain amide linkages between the PEG and the porphyrin macrocycle (Scheme 1). In order to overcome the low nucleophilicity of the aminophenyl-porphyrins and the steric effects imposed by the porphyrin

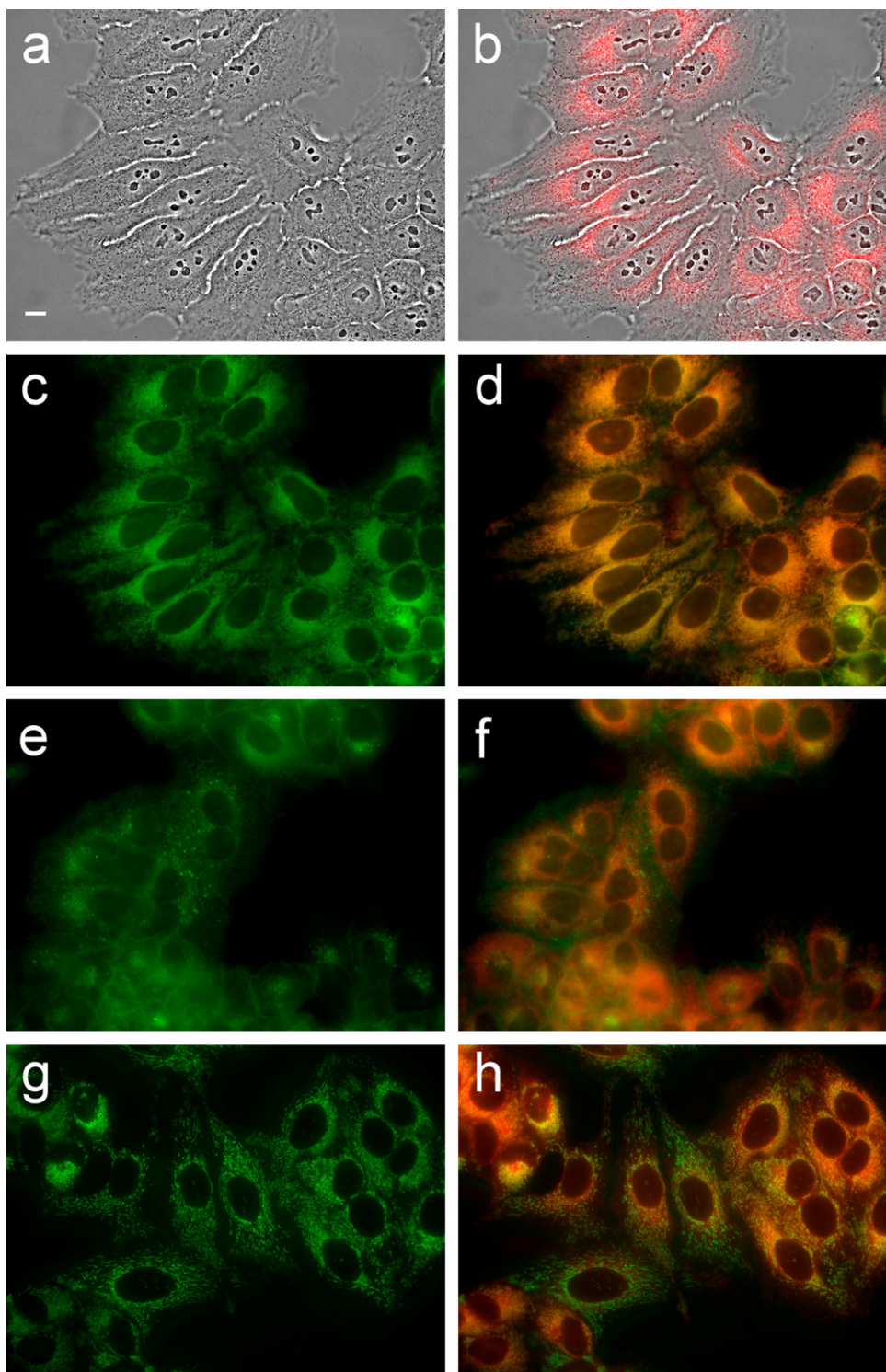


Fig. 6. Subcellular localization of conjugate **7** in HEp2 cells at 10 μM for 18 h: (a) phase contrast, (b) overlay of **7** fluorescence and phase contrast, (c) DiOC₆ fluorescence, (e) LysoSensor Green fluorescence, (g) MitoTracker Green fluorescence, (d), (f) (h) overlays of organelle tracers with **7** fluorescence. Scale bar: 10 μm .

ring, the amino groups were converted into the carboxylic acids **2–5** upon reaction with glycolic anhydride. This reaction proceeds smoothly at room temperature and in excellent yields (93–100%) when a 1:1.5 ratio of aminoporphyrin/glycolic anhydride is used. The pegylation of porphyrins **2–5** was performed in solution-phase using

our previously reported conjugation methodologies, with HOBt and EDCI as the coupling agents [38]. The *tert*-butyl-protected PEG-porphyrins were isolated in 40–64% yields after purification using flash chromatography on silica gel. Deprotection upon treatment with TFA at room temperature gave PEG-porphyrins **6–9** in quantitative

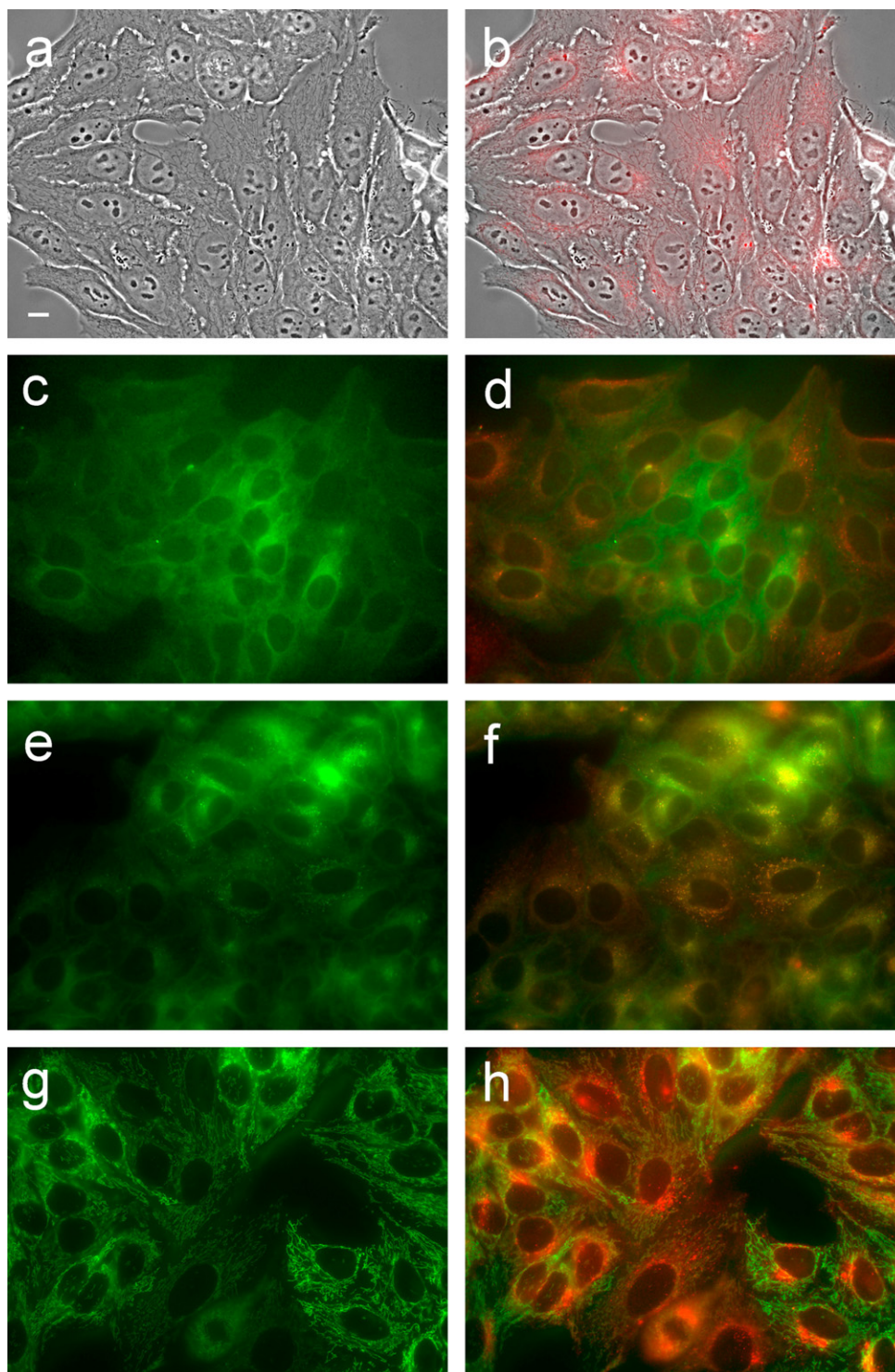


Fig. 7. Subcellular localization of conjugate **8** in Hep2 cells at 10 μM for 18 h: (a) phase contrast, (b) overlay of **8** fluorescence and phase contrast, (c) DiOC₆ fluorescence, (e) LysoSensor Green fluorescence, (g) MitoTracker Green fluorescence, (d), (f) (h) overlays of organelle tracers with **8** fluorescence. Scale bar: 10 μm .

yields. The hydrophobic character of the PEG-porphyrins **6–9**, as determined by their retention times on a reverse-phase HPLC column, decreases in the order $6 > 7 > 8 > 9$. Indeed, while the more hydrophobic PEG-porphyrins **6** and **7** were soluble in organic solvents and poorly soluble in water, porphyrins **8** and **9** were highly soluble in both

water and polar organic solvents. The fluorescence emission properties of the PEG-porphyrins (Fig. 1) suggest that porphyrins **8** and **9** have a stronger tendency for aggregation in buffered aqueous solution (in 50 mM HEPES buffer, pH 7.4) than the more hydrophobic porphyrins **6** and **7** due to their larger number of PEG linkages.

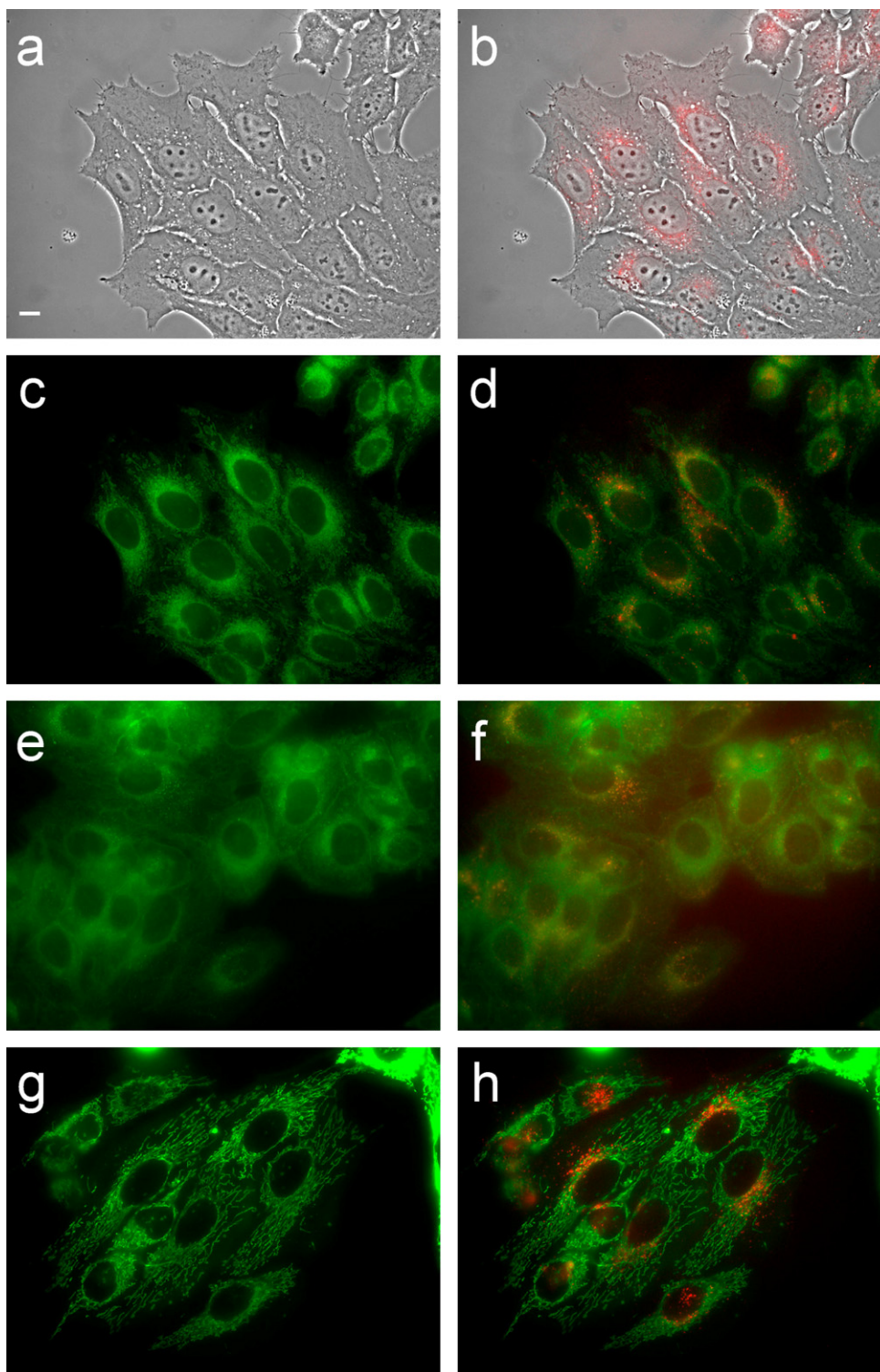


Fig. 8. Subcellular localization of conjugate **9** in HEp2 cells at 10 μ M for 18 h: (a) phase contrast, (b) overlay of **9** fluorescence and phase contrast, (c) DiOC₆ fluorescence, (e) LysoSensor Green fluorescence, (g) MitoTracker Green fluorescence, (d), (f) (h) overlays of organelle tracers with **9** fluorescence. Scale bar: 10 μ m.

4.2. Cellular studies

The biological properties of the PEG-porphyrins **6–9** depend on the number of PEG chains linked to the porphyrin periphery. The least hydrophobic porphyrins **8** and **9**

were taken up faster during the first 1–2 h than the more hydrophobic porphyrins **6** and **7**, but after 2 h a plateau was reached (Fig. 2). In contrast, porphyrins **6** and **7** steadily continued to accumulate within cells over the 24 h period studied, and after this time approximately 12 times

more **6** and **7** were found within cells than **8** or **9**. We believe that the cellular uptake of our series of PEG-porphyrins depends on their hydrophobic character, as has been previously reported for porphyrin-based photosensitizers [43,44], and also on their aggregation behavior. Porphyrins **8** and **9** might be too hydrophilic to efficiently interact and cross the lipid bilayer of plasma membranes, while **6** and **7** have a more favorable lipophilic/hydrophilic balance. We believe that the amphiphilicity conferred by the mono-PEG- and the adjacent di-PEG-substitution at the porphyrin periphery enhances the affinity of porphyrins **6** and **7** for lipid/aqueous interfaces, therefore favoring cellular uptake. On the other hand, our results indicate that porphyrins containing more than two low molecular PEG chains, i.e. PEG-porphyrins **8** and **9**, show increased tendency to form aggregates in buffered aqueous solution, and that this tendency is particularly significant in the case of the symmetric tetra-PEG-porphyrin **9**. The resulting aggregates, presumably of large size due to their self-association and binding of multiple water molecules [23], have decreased tendency for crossing plasma membranes and consequently lower cellular uptake. It might also be possible that the overall negative charge of the PEG-porphyrins, due to their terminal carboxylic acid groups, also plays a role on their uptake into cells. It has been observed that the plasma membrane of mammalian and tumor cells contain higher net negative charge compared with normal cells, due to the overexpression of polysialic acid residues [45]. Therefore, as the number of PEG groups and consequently negative charges increases on the PEG-porphyrins, the repulsive interactions with the anionic regions of the plasma membrane may increase, resulting in lower cellular uptake.

All PEG-porphyrins showed no dark cytotoxicity up to 250 μM concentrations, in human HEP2 cells (Fig. 3). However, upon activation with low light dose (1 J/cm²) PEG-porphyrins **6** and **7** bearing one and two PEG chains, respectively, exhibited high toxicity with determined IC₅₀ values of 2.0 and 1.8 μM , respectively (Fig. 4). The observed phototoxic effect of porphyrins **6** and **7** is probably due to both their high cellular uptake (Fig. 2) and their preferential subcellular localization within the sensitive cell organelles mitochondria and ER (Figs. 5 and 6). Porphyrin-mediated mitochondria and ER photodamage can lead to rapid cell death via apoptosis and consequently to preferential phototoxicity [46–49]. On the other hand PEG-porphyrins **8** and **9** were found preferentially within vesicles that correlated well with the cell lysosomes. These results suggest that PEG-porphyrins **8** and **9** are probably taken up by cells via an endocytic pathway while **6** and **7** might interact in multiple ways with the plasma membranes and consequently follow several uptake mechanisms [4]. Another possible reason for the observed non-toxicity of porphyrins **8** and **9** is their tendency for aggregation, which might result in reduction of their ability to produce singlet oxygen. The possible inactivation of singlet oxygen by PEG chains has been previously reported [28,50].

5. Conclusions

A series of PEG-functionalized porphyrins bearing one to four low molecular weight PEG chains has been synthesized in good overall yields from the corresponding readily available amino-substituted porphyrins. The hydrophobic character of the PEG-porphyrins decreased with the number of PEG chains at the macrocycle periphery while their tendency for aggregation increased with the number of PEG chains. All PEG-porphyrins were found to be non-toxic in the dark up to 250 μM concentrations and only the PEG-porphyrins bearing one or two PEG chains were phototoxic (IC₅₀ 2.0 and 1.8 μM , respectively, at 1 J/cm² light dose). Our results show that the cellular properties of PEG-substituted porphyrins depend on the number of PEG chains linked to the porphyrin ring; more than two PEG chains increase the hydrophilicity of the photosensitizers, their aggregation in aqueous solution, and reduces their cellular uptake and phototoxicity. On the other hand, amphiphilic photosensitizers bearing one or two PEG chains, the latter on the same side of the macrocycle, were efficiently taken up by cells, localized preferentially in sensitive organelles (mitochondria and ER) and were highly phototoxic.

Acknowledgements

The work described was supported by the National Science Foundation, grant number CHE-304833.

References

- [1] T.J. Dougherty, C.J. Gomer, B.W. Henderson, G. Jori, D. Kessel, M. Korbelik, J. Moan, Q. Peng, Photodynamic therapy, *J. Natl. Cancer Inst.* 90 (1998) 889–905.
- [2] R.K. Pandey, G. Zheng, Porphyrins as photosensitizers in photodynamic therapy, in: K.M. Kadish, K.M. Smith, R. Guilard (Eds.), *The Porphyrin Handbook*, Academic Press, Boston, 2000, pp. 157–230.
- [3] N. Oku, N. Saito, Y. Namba, H. Tsukada, D. Solphin, S. Okada, Application of long-circulating liposomes to cancer photodynamic therapy, *Biol. Pharm. Bull.* 20 (1997) 670–673.
- [4] J. Osterloh, M.G.H. Vicente, Mechanisms of porphyrinoid localization in tumors, *J. Porphyrins Phthalocyanines* 6 (2002) 305–324.
- [5] (a) M.R. Hamblin, E.L. Newman, Photosensitizer targeting in photodynamic therapy. I. Conjugates of haematoporphyrin with albumin and transferrin, *J. Photochem. Photobiol. B: Biol.* 26 (1994) 45–56;
(b) M.R. Hamblin, E.L. Newman, Photosensitizer targeting in photodynamic therapy. II. Conjugates of haematoporphyrin with serum lipoproteins, *J. Photochem. Photobiol. B: Biol.* 26 (1994) 147–157.
- [6] A.E. Soini, D.V. Yashunsky, N.J. Meltola, G.V. Ponomarev, Influence of linker unit on performance of palladium(II) coproporphyrin labelling reagent and its bioconjugates, *Luminescence* 18 (2003) 182–192.
- [7] A.V. Chudinov, V.D. Rumiantseva, A.V. Lobanov, G.K. Chudinova, A.A. Stomakhin, A.F. Mironov, Synthesis of conjugates of bovine serum albumin with water-soluble ytterbium porphyrins, *Bioorg. Khim.* 30 (2004) 99–104.
- [8] (a) B. Mestre, A. Jakobs, G. Pratviel, B. Meunier, Structure/nuclease activity relationships of DNA cleavers based on cationic metalloporphyrin-oligonucleotide conjugates, *Biochemistry* 35 (1996) 9140–9149;

- (b) B. Mestre, M. Pitie, C. Loup, C. Claparols, G. Pratiel, B. Meunier, Influence of the nature of the porphyrin ligand on the nuclease activity of metalloporphyrin-oligonucleotide conjugates designed with cationic, hydrophobic or anionic metalloporphyrins, *Nucleic Acids Res.* 25 (1997) 1022–1027.
- [9] H. Li, O.S. Fedorova, W.R. Trumble, T.R. Fletcher, L. Czuchajowski, Site-specific photomodification of DNA by porphyrin-oligonucleotide conjugates synthesized via a solid phase H-phosphonate approach, *Bioconjugate Chem.* 8 (1997) 49–56.
- [10] C.H. Bedel-Cloutour, L. Mauclair, A. Saux, M. Pereyre, Syntheses of functionalized indium porphyrins for monoclonal antibody labeling, *Bioconjugate Chem.* 7 (1996) 617–627.
- [11] (a) M. Del Governatore, M.R. Hamblin, E.E. Piccinini, G. Ugolini, T. Hasan, Targeted photodestruction of human colon cancer cells using charged 17.1A chlorin e_6 immunoconjugates, *Br. J. Cancer* 82 (2000) 56–64;
(b) M.R. Hamblin, M. Del Governatore, I. Rizvi, T. Hasan, Biodistribution of charged 17.1A photoimmunoconjugates in a murine model of hepatic metastasis of colorectal cancer, *Br. J. Cancer* 83 (2000) 1544–1551.
- [12] R. Hudson, M. Carcenac, K. Smith, L. Madden, O.J. Clarke, A. Pelegrin, J. Greenman, R.W. Boyle, The development and characterization of porphyrin isothiocyanate-monoclonal antibody conjugates for photoimmunotherapy, *Br. J. Cancer* 92 (2005) 1442–1449.
- [13] (a) A. Gijssens, P. Witte, Photocytotoxic action of EGF-PVA-Sn(IV)chlorin e_6 and EGF-dextran-Sn(IV)chlorin e_6 internalizable conjugates on A431 cells, *Int. J. Oncol.* 13 (1998) 1171–1177;
(b) A. Gijssens, L. Missiaen, W. Merlevede, P. Witte, Epidermal growth factor-mediated targeting of chlorin e_6 selectively potentiates its photodynamic activity, *Cancer Res.* 60 (2000) 2197–2202.
- [14] A.A. Savitsky, N.V. Gukasova, S.G. Gumanov, N.B. Feldman, E.A. Luk'yanets, A.F. Mironov, R.I. Yakubovskaya, S.V. Lutsenko, S.E. Severin, Cytotoxic action of conjugates of alpha-fetoprotein and epidermal growth factor with photoheme, chlorines, and phthalocyanines, *Biochemistry (Moscow)* 65 (2000) 732–736.
- [15] X. Chen, L. Hui, D.A. Foster, C.M. Drain, Efficient synthesis and photodynamic activity of porphyrin-saccharide conjugates: targeting and incapacitating cancer cells, *Biochemistry* 43 (2004) 10918–10929.
- [16] G. Li, S.K. Pandey, A. Graham, M.P. Dobhal, R. Mehta, Y. Chen, A. Gryshuk, K. Rittenhouse-Olson, A. Oseroff, R.K. Pandey, Functionalization of OEP-based benzochlorins to develop carbohydrate-conjugated photosensitizers. Attempt to target beta-galactoside-recognized proteins, *J. Org. Chem.* 69 (2004) 158–172.
- [17] (a) N.S. Soukos, M.R. Hamblin, T. Hasan, The effect of charge on cellular uptake and phototoxicity of polylysine chlorin(e_6) conjugates, *Photochem. Photobiol.* 65 (1997) 723–729;
(b) M.R. Hamblin, D.A. O'Donnell, N. Murthy, K. Rajagopalan, N. Michaud, M.E. Sherwood, T. Hasan, Polycationic photosensitizer conjugates: effects of chain length and Gram classification on the photodynamic inactivation of bacteria, *J. Antimicrob. Chemother.* 49 (2002) 941–951.
- [18] (a) J.M. Lu, C.M. Peterson, J. Guo-Shiah, Z.W. Gu, C.A. Peterson, R.C. Straight, J. Kopecek, Cooperativity between free and *N*-(2-hydroxypropyl)methacrylamide copolymer bound adriamycin and *meso*-chlorin e_6 monoethylene diamine induced photodynamic therapy in human epithelial ovarian carcinoma in vitro, *Int. J. Oncol.* 15 (1999) 5–16;
(b) V. Omelyanenko, C. Gentry, P. Kopeckova, J. Kopecek, HPMA copolymer-anticancer drug-OV-TL16 antibody conjugates. II. Processing in epithelial ovarian carcinoma cells in vitro, *Int. J. Cancer* 75 (1998) 600–608.
- [19] (a) M. Tijerina, P. Kopeckova, J. Kopecek, Mechanisms of cytotoxicity in human ovarian carcinoma cells exposed to free Mce6 or HPMA copolymer-Mce6 conjugates, *Photochem. Photobiol.* 77 (2003) 645–652;
(b) M. Tijerina, P. Kopeckova, J. Kopecek, Correlation of subcellular compartmentalization of HPMA copolymer-Mce6 conjugates with chemotherapeutic activity in human ovarian carcinoma cells, *Pharm. Res.* 20 (2003) 728–737.
- [20] S. Zalipsky, Chemistry of polyethylene glycol conjugates with biologically active molecules, *Adv. Drug Deliv. Rev.* 16 (1995) 157–182.
- [21] M.J. Roberts, M.D. Bentley, J.M. Harris, Chemistry for peptide and protein PEGylation, *Adv. Drug Deliv. Rev.* 54 (2002) 459–476.
- [22] (a) R.B. Greenwald, PEG drugs: an overview, *J. Control Release* 74 (2001) 159–171;
(b) R.B. Greenwald, Y.H. Choe, J. McGuire, C.D. Conover, Effective drug delivery by PEGylated drug conjugates, *Adv. Drug Deliv. Rev.* 55 (2003) 217–250.
- [23] M.R. Hamblin, J.L. Miller, I. Rizvi, H.G. Loew, T. Hasan, Pegylation of charged polymer-photosensitizer conjugates: effects on photodynamic therapy, *Br. J. Cancer* 89 (2003) 937–943.
- [24] (a) R. Hornung, M.K. Fehr, J. Monti-Frayne, B.J. Tromberg, M.W. Berns, Y. Tadir, Minimally-invasive debulking of ovarian cancer in the rat pelvis by means of photodynamic therapy using the pegylated photosensitizer PEG-m-THPC, *Br. J. Cancer* 81 (1999) 631–637;
(b) R. Hornung, M.K. Fehr, H. Walt, P. Wyss, M.W. Berns, Y. Tadir, PEG-m-THPC-mediated photodynamic effects on normal rat tissues, *Photochem. Photobiol.* 72 (2000) 696–700.
- [25] P. Westerman, T. Glanzmann, S. Andrejevic, D.R. Braichotte, M. Forrer, G.A. Wagnier, P. Monnier, H. van den Bergh, J.P. Mach, S. Folli, Long circulating half-life and high tumor selectivity of the photosensitizer meta-tetrahydroxyphenylchlorin conjugated to polyethylene glycol in nude mice grafted with a human colon carcinoma, *Int. J. Cancer* 76 (1998) 842–850.
- [26] J.P. Rovers, A.E. Saarnak, M. de Jode, H.J. Sterenberg, O.T. Terpstra, M.F. Grahn, Biodistribution and bioactivity of tetra-pegylated *meta*-tetra(hydroxyphenyl)chlorin compared to native *meta*-tetra(hydroxyphenyl)chlorin in a rat liver tumor model, *Photochem. Photobiol.* 71 (2000) 211–217.
- [27] O. Bourdon, V. Mosqueira, P. Legrand, J. Blais, A comparative study of the cellular uptake, localization and phototoxicity of *meta*-tetra(hydroxyphenyl) chlorin encapsulated in surface-modified sub-micronic oil/water carriers in HT29 tumor cells, *J. Photochem. Photobiol. B: Biol.* 55 (2000) 164–171.
- [28] T. Reuther, A.C. Kubler, U. Zillmann, C. Flechtenmacher, H. Sinn, Comparison of the in vivo efficiency of photofrin II-, mTHPC-, mTHPC-PEG- and mTHPCnPEG-mediated PDT in a human xenografted head and neck carcinoma, *Lasers Surg. Med.* 29 (2001) 314–322.
- [29] T. Krueger, H.J. Altermatt, D. Mettler, B. Scholl, L. Magnusson, H.B. Ris, Experimental photodynamic therapy for malignant pleural mesothelioma with pegylated mTHPC, *Lasers Surg. Med.* 32 (2003) 61–68.
- [30] S.K. Sahoo, T. Sawa, J. Fang, S. Tanaka, Y. Miyamoto, T. Akaike, H. Maeda, Pegylated zinc protoporphyrin: a water-soluble heme oxygenase inhibitor with tumor-targeting capacity, *Bioconjugate Chem.* 13 (2002) 1031–1038.
- [31] (a) J. Fang, T. Sawa, T. Akaike, T. Akuta, S.K. Sahoo, G. Khaled, A. Hamada, H. Maeda, In vivo antitumor activity of pegylated zinc protoporphyrin: targeted inhibition of heme oxygenase in solid tumor, *Cancer Res.* 63 (2003) 3567–3574;
(b) J. Fang, T. Sawa, T. Akaike, K. Greish, H. Maeda, Enhancement of chemotherapeutic response of tumor cells by a heme oxygenase inhibitor, pegylated zinc protoporphyrin, *Int. J. Cancer* 109 (2004) 1–8.
- [32] Y. Kodera, A. Ajima, K. Takahashi, A. Matsushima, Y. Saito, Y. Inada, Polyethylene glycol-modified hematoporphyrin as photosensitizer, *Photochem. Photobiol.* 47 (1988) 221–223.
- [33] C. Lottner, R. Kneuchel, G. Bernhardt, H. Brunner, Distribution and subcellular localization of a water-soluble hematoporphyrin-platinum(II) complex in human bladder cancer cells, *Cancer Lett.* 215 (2004) 167–177.
- [34] P.J. Stevens, M. Sekido, R.J. Lee, Synthesis and evaluation of a hematoporphyrin derivative in a folate receptor-targeted solid-lipid nanoparticle formulation, *Anticancer Res.* 24 (2004) 161–165.

- [35] M.D. Savellano, T. Hasan, Targeting cells that overexpress the epidermal growth factor receptor with polyethylene glycolated BPD verteporfin photosensitizer immunoconjugates, *Photochem. Photobiol.* 77 (2003) 431–439.
- [36] J.X. Zhang, C.B. Hansen, T.M. Allen, A. Boey, R. Boch, Lipid-derivatized poly(ethylene glycol) micellar formulations of benzoporphyrin derivatives, *J. Control Release* 86 (2003) 323–338.
- [37] K. Ichikawa, T. Hikita, N. Maeda, Y. Takeuchi, Y. Namba, N. Oku, PEGylation of liposome decreases the susceptibility of liposomal drug in cancer photodynamic therapy, *Biol. Pharm. Bull.* 27 (2004) 443–444.
- [38] M. Sibrian-Vazquez, T.J. Jensen, R.P. Hammer, M.G.H. Vicente, Peptide-mediated cell transport of water soluble porphyrin conjugates, *J. Med. Chem.* 49 (2006) 1364–1372.
- [39] R. Luguya, L. Jaquinod, F.R. Fronczek, M.G.H. Vicente, K.M. Smith, Synthesis and reactions of *meso*-(*p*-nitrophenyl)porphyrins, *Tetrahedron* 60 (2004) 2757–2763.
- [40] R. Lauceri, R. Purrello, S.J. Shetty, M.G.H. Vicente, Interactions of anionic carboranated porphyrins with DNA, *J. Am. Chem. Soc.* 123 (2001) 5835–5836.
- [41] J.M. Ribo, J. Crusats, J.-A. Farrera, M.L. Valero, Aggregation in water solutions of tetrasodium diprotonated *meso*-tetrakis(4-sulfonatophenyl)porphyrin, *J. Chem. Soc. Chem. Commun.* (1994) 681–682.
- [42] M.F. Grahn, A. Giger, A. McGuinness, M.L. de Jode, J.C.M. Stewart, H.-B. Ris, H.J. Altermatt, N.S. Williams, mTHPC polymer conjugates: the in vivo photodynamic activity of four candidate compounds, *Lasers Med. Sci.* 14 (1999) 40–46.
- [43] K.W. Woodburn, N.J. Vardaxis, J.S. Hill, A.H. Kaye, J.A. Reiss, D.R. Phillips, Evaluation of porphyrin characteristics required for photodynamic therapy, *Photochem. Photobiol.* 55 (1992) 697–704.
- [44] B.W. Henderson, D.A. Bellnier, W.R. Greco, A. Sharma, R.K. Pandey, L.A. Vaughan, K.R. Weishaupt, T.J. Dougherty, An in vivo quantitative structure–activity relationship for a congeneric series of pyropheophorbide derivatives as photosensitizers for photodynamic therapy, *Cancer Res.* 57 (1997) 4000–4007.
- [45] S.E. Kornguth, T. Kalianke, H.I. Robins, J.D. Cohen, P. Turski, Preferential binding of radiolabeled poly-L-lysine to C6 and U87 MG glioblastomas compared to endothelial cells in vitro, *Cancer Res.* 49 (1989) 6390–6395.
- [46] Y. Luo, C.K. Chang, D. Kessel, Rapid initiation of apoptosis by photodynamic therapy, *Photochem. Photobiol.* 63 (1996) 528–534.
- [47] D. Kessel, Y. Luo, Mitochondrial photodamage and PDT-induced apoptosis, *J. Photochem. Photobiol. B: Biol.* 42 (1998) 89–95.
- [48] D. Kessel, Correlation between subcellular localization and photodynamic efficacy, *J. Porphyrins Phthalocyanines* 8 (2004) 1009–1014.
- [49] R.V. Rao, E. Hermel, S. Castro-Obregon, G. del Rio, L.M. Ellerby, H.M. Ellerby, D.E. Bredesen, Coupling endoplasmic reticulum stress to the cell death program. Mechanism of caspase activation, *J. Biol. Chem.* 276 (2001) 33869–33874.
- [50] J.R. Kanofsky, Quenching of singlet oxygen by human plasma, *Photochem. Photobiol.* 51 (1990) 299–303.